Available online at www.sciencedirect.com
SCIENCE DIRECT®
ELSEVIER
International Journal of Machine Tools & Manufacture 44 (2004) 391–400
INTERNATIONAL JOURNAL OF MACHINE TOOLS & MANUFACTURE DESIGN, RESEARCH AND APPLICATION
www.elsevier.com/locate/ijmatool

Investigation of the spark cycle on material removal rate in wire electrical discharge machining of advanced materials

Scott F. Miller [a], Albert J. Shih [a,*], Jun Qu [b]

[a] Department of Mechanical Engineering, University of Michigan, Ann Arbor, MI 48109, USA
[b] Oak Ridge National Laboratory, Oak Ridge, TN 37831, USA

Received 21 August 2003; received in revised form 23 September 2003; accepted 15 October 2003

Abstract

The development of new, advanced engineering materials and the need for precise and flexible prototypes and low-volume production have made the wire electrical discharge machining (EDM) an important manufacturing process to meet such demands. This research investigates the effect of spark on-time duration and spark on-time ratio, two important EDM process parameters, on the material removal rate (MRR) and surface integrity of four types of advanced material: porous metal foams, metal bond diamond grinding wheels, sintered Nd-Fe-B magnets, and carbon–carbon bipolar plates. An experimental procedure was developed. During the wire EDM, five types of constraints on the MRR due to short circuit, wire breakage, machine slide speed limit, and spark on-time upper and lower limits are identified. An envelope of feasible EDM process parameters is generated for each work-material. Applications of such a process envelope to select process parameters for maximum MRR and for machining of micro features are discussed. Results of Scanning Electron Microscopy (SEM) analysis of surface integrity are presented.

Keywords: Electrical discharge machining; Material removal rate; Surface integrity

1. Introduction

The development of new, advanced engineering materials and the need for precise and flexible prototypes and low-volume component production have made EDM an important manufacturing process to meet such a demand. The wire EDM process uses electrical sparks between a thin, traveling wire electrode and the workpiece to erode the work-material and generate the desired shape. The force generated in EDM is small, which makes it suitable for cutting porous foam materials, carbon–carbon bipolar plate, and manufacturing of miniature features in micro-mechanical components. By adding a rotary spindle to the wire EDM machine, this process can be used to machine cylindrical parts and to shape the metal bond diamond grinding wheels.

Information for the selection of proper process parameters for wire EDM of newly developed materials, such as the machining of advanced engineering materials, micro-fabrication, truing of metal bond diamond wheels and others, is not readily available. For a commercial EDM machine, the manufacturer provides a database of setup parameters for commonly used work- and electrode-materials under typical operating conditions. Such a database cannot meet the growing new EDM applications, including machining new advanced materials and miniature features. The goal of this study is to investigate the effect of spark on-time duration and spark on-time ratio, two important wire EDM process parameters, on the truing of metal bond diamond wheels and machining of new engineering materials: porous metal foams, sintered Nd-Fe-B magnets, and carbon–carbon fuel cell bipolar plates. An envelope of MRR is generated for the selection of process parameters for each material.

Effects of EDM process parameters have been investigated. Wang and Yan [1], Lin et al. [2] and Lin and Lin [3] studied the effect of current, polarity, voltage, and spark on-time on the EDM process by using the Taguchi method. Uno et al. [4] showed relationships between the material removal rate and spark on-time in

* Corresponding author. Tel.: +1-734-647-1766; fax: +1-734-936-0363.
E-mail address: shiha@umich.edu (A.J. Shih).

0890-6955/$ - see front matter © 2003 Elsevier Ltd. All rights reserved.
doi:10.1016/j.ijmachtools.2003.10.005

EDM of silicon and mild steel. Tsai and Wang [5] compared the neutral network models on material removal rate in EDM. Lee and Li [6] studied the effects of process parameters in EDM of tungsten carbide. Hocheng et al. [7] investigated the correlation of current and spark on-time and the crater size produced by a single spark of SiC/Al work-material. Qu et al. [8,9] examined the EDM process parameters in a cylindrical EDM process. This survey found the lack of research in EDM of newly developed engineering materials and the boundaries that limits the MRR in wire EDM. This research investigates the effect of spark on-time duration and spark on-time ratio, two important EDM process parameters, on the surface finish characteristics and integrity of four types of advanced engineering material: porous metal foams, metal bond diamond grinding wheels, sintered Nd-Fe-B magnets, and carbon–carbon bipolar plates.

An envelope of feasible wire EDM process parameters is identified for each work-material. This envelope can be applied to setup the EDM process for efficient, high MRR machining. A rough surface with a thick recast layer is usually generated in high MRR EDM. Another application of the wire EDM envelope is the selection of process parameters for slow, low MRR EDM cutting to generate better surface roughness and enable the machining of micro-features.

The setup of the wire EDM machine and experimental procedure are first discussed. Work-materials investigated in this study are introduced. Experimental and regression modeling results as well as envelopes of feasible EDM process for different work-materials are then presented. Finally, the EDM surfaces are studied using the scanning electron microscopy (SEM).

2. Experimental setup and work-materials

2.1. Wire EDM machine setup

The EDM experiments were conducted on a Brother HS-5100 wire EDM machine. A copper wire with 0.25 mm nominal diameter was used. Two wire EDM configurations were studied. One is slicing a solid plate or foam material. The workpiece was immersed in the deionized water with high pressure waterjets flushing to remove debris in the gap between the wire electrode and workpiece. Fig. 1 shows the setup to cut a metal foam plate. The other configuration was the wire EDM of rotating grinding wheels. This concept has been demonstrated by Rhoney et al. [10].

Two EDM process parameters studied were the spark cycle, T, and spark-on time, T_{on}. Fig. 2 shows the ideal waveform of voltage between the workpiece and wire electrode during EDM. The spark cycle, T, is the period of change in voltage. The spark on-time or pulse on-time, T_{on}, is the duration in a spark cycle that the voltage has been built up. For the Brother HS-5100 EDM machine, the range for spark cycle (T) is from 10 to 1000 μs, and for spark on-time (T_{on}) is from 2 to 18 μs. The wire feed speed is set at 15 mm/s, wire tension is 0.15 N, and the gap voltage between the wire and electrode is set at 35 V.

Fig. 1. Setup of the wire EDM machining of a metal foam plate.

2.2. Work-materials

Six work-materials, including two metal foams, two diamond grinding wheels, one sintered Nd-Fe-B magnet, and one carbon–carbon bipolar plate, were investigated in this study.

2.2.1. Metal foams

Two types of metal foams are studied. One is the Fe-Cr-Al alloy, also known as Fecralloy or Kanthal. This is a high temperature oxidation resistance foam, as shown in Fig. 3(a). This foam material can withstand an operation temperature in excess of 1200 °C and is popular for heat exchanger applications. Another metal foam work-material is the 316 stainless steel foam, as

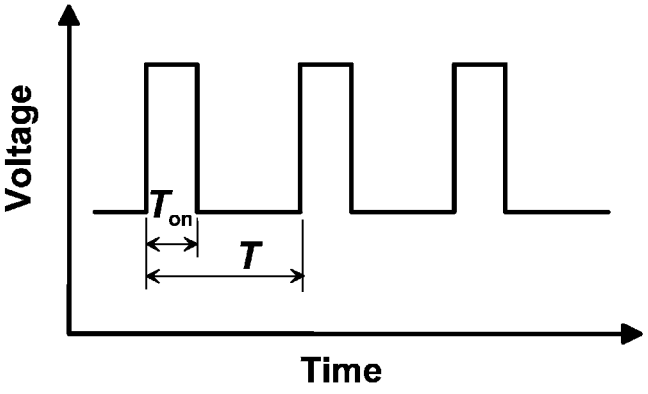

Fig. 2. Definition of the spark cycle, T, and spark on-time, T_{on}, in the EDM spark cycle.

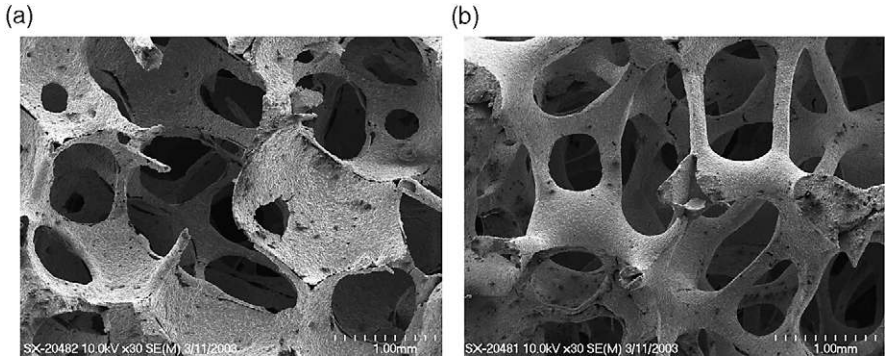

Fig. 3. EDM cut porous metal foam (a) Fe-Cr-Al foam and (b) 316 stainless steel foam.

shown in Fig. 3(b). The foam structure, as shown in the SEM micrograph in Fig. 3, consists of ligaments creating a network of inter-connected, dodecahedral-shaped cells. The cells are randomly oriented and mostly uniform in size and shape. The ligaments are hollow with a triangular-shaped hole, a result of the manufacturing technique used. The metal foams were produced using open-cell polyurethane foam as templates [11,12]. The Fe-Cr-Al alloy and 316 stainless steel powder slurry was coated onto the polyurethane foam and fired in a kiln. The polyurethane foam was burned out during the firing, leaving the triangular-shaped hollow hole inside each of the ligaments. The Fe-Cr-Al and 316 stainless steel foams used in this study have a pore size of 30 ppi (pores per inch) and 5.1 and 6.9 wt% density, respectively. The thickness of metal foam plate, as seen in Fig. 1, is 25 mm.

2.2.2. Diamond grinding wheels

The wire EDM process can be used to create an intricate shape on a rotating metal bond diamond wheel for precision form grinding of ceramics and other difficult-to-machine materials [10]. This study investigated the effect of T and T_{on} on MRR. The high MRR setup is used at the start of the truing process to rapidly create the rough form on the grinding wheel. In final truing paths, the set of EDM process parameters that enable the creation of intricate forms is applied.

Two bronze bond diamond grinding wheels, denoted as wheel I and II, were used in this study. Wheel I, 200 mm in diameter and manufactured by Norton Saint-Gobain with tradename of Scepter, has the 320 ANSI mesh size diamond (average abrasive size of 54 μm). Wheel II (Inland MD1200N50M-1/4) has the very fine, 1200 ANSI mesh diamond (average abrasive size about 8 μm).

2.2.3. Sintered Nd-Fe-B permanent magnet

The sintered Nd-Fe-B permanent magnets are Neomag 34KC2, supplied by Magnequench. This nanocrystalline Nd-Fe-B powder is sintered by the hot-isostatic press and then magnetized to become a permanent magnet. EDM tests were conducted on the sintered material that had not yet been magnetized. The rare-earth Nd-Fe-B magnet has high magnetic density and is used extensively for miniature, energy-efficient electrical motor, actuator, and generator applications. In this study, the 27 mm thick Nd-Fe-B plate was used to study the effect of T and T_{on} on MRR and surface integrity.

2.2.4. Carbon–carbon bipolar plate

The carbon–carbon bipolar plate, provided by Porvair LLC, has been developed for proton exchange membrane (PEM) fuel cell applications. This material uses slurry molded carbon fiber, about 0.4 mm long and 0.01 mm in diameter, sealed with chemically vapor-infiltrated carbon [13]. The material has good electrical conductivity, 0.4 $\Omega.cm^2$ at 1.15 A/cm^2 and 0.9 $\Omega.cm^2$ at 0.05 A/cm^2 current. A plate of 2.3 mm thickness was used in this study.

2.3. Experimental procedure

The maximum MRR in wire EDM is constrained by the machine, tooling, and physical limitations. Sets of EDM test were first conducted under specific pulse on-time, T_{on}, at 4, 6, 10, 14, and 18 μs. For the wire EDM machine used in this study, 2 and 18 μs is the lower and upper limit for T_{on}, respectively. Under the same T_{on}, the spark cycle, T, was varied to achieve different T_{on}/T ratio. Without knowing the behavior of the new work-materials processed by EDM, different levels of T were tested. The wire EDM machine automatically increases or decreases the wire feed speed to maintain the target gap voltage. The steady-state wire feed rate is recorded and converted to the MRR.

When T is low, a limit is reached when the electrical spark energy is strong and the wire electrode cannot withstand the high energy density and frequently breaks during cutting. At the other extreme, when T is high, the electrical spark is rare and the wire frequently

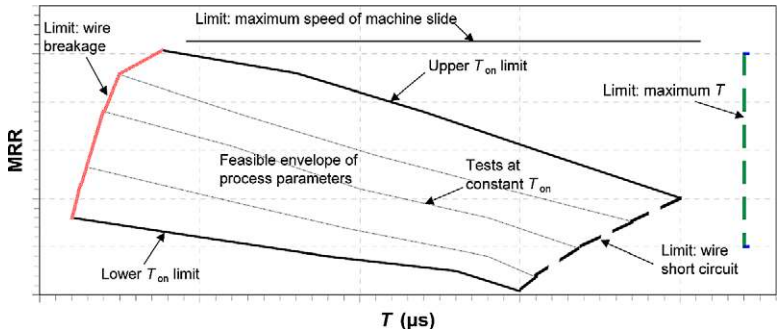

Fig. 4. Machine limits and boundaries for a feasible wire EDM process envelope.

touches the workpiece and shorts the electrical circuit for spark generation. Tests at different T were conducted to find these two extreme cases to extract the wire feed rate for a specific T_{on}. The MRR is usually high at lower T.

A typical envelope of feasible material removal rate is shown in Fig. 4. The wire feed rate vs. T curves can be generated for each T_{on}. The envelope is enclosed by four sides: the top and bottom are the upper and lower limit of T_{on}, 18 and 2 μs for the wire EDM machine used in this study, respectively, and left and right are the wire breakage and wire short circuit limits, respectively. It is noted that steady-state EDM cutting at 2 or 4 μs T_{on} is difficult to reach. The lowest T_{on} is usually at 4 or 6 μs. The wire feed rate is restricted by the machine slide speed limit, which is 305 mm/min, and the spark cycle is limited to 1000 μs for the Brother-5100 wire EDM machine used in this study. The horizontal and vertical boundary lines in Fig. 4 show these two limits.

3. Experimental results of wire EDM material removal rate

3.1. Metal foams

Fig. 5 shows three envelopes of feasible T and T_{on} for wire EDM cutting of 316 stainless steel and Fe-Cr-Al foam and a low carbon steel plate with comparative effective thickness (1.57 mm) to metal foams. Five sets of tests at 4, 6, 10, 14, and 18 μs T_{on} were conducted on the three materials. Each set of tests is represented by a line with different symbols to represent test points. The 2 μs T_{on} was tried but failed to achieve the steady-state EDM condition. The 18 and 4 μs T_{on} are the upper and low limits on the envelope. On the left is the limit of wire breakage. On the right is the limit of wire short circuit. The wire feed rate was slow enough that the machine slide speed limit was not a constraint. It is important to point out that the wire short circuit and breakage limits are not exact. There exist two narrow

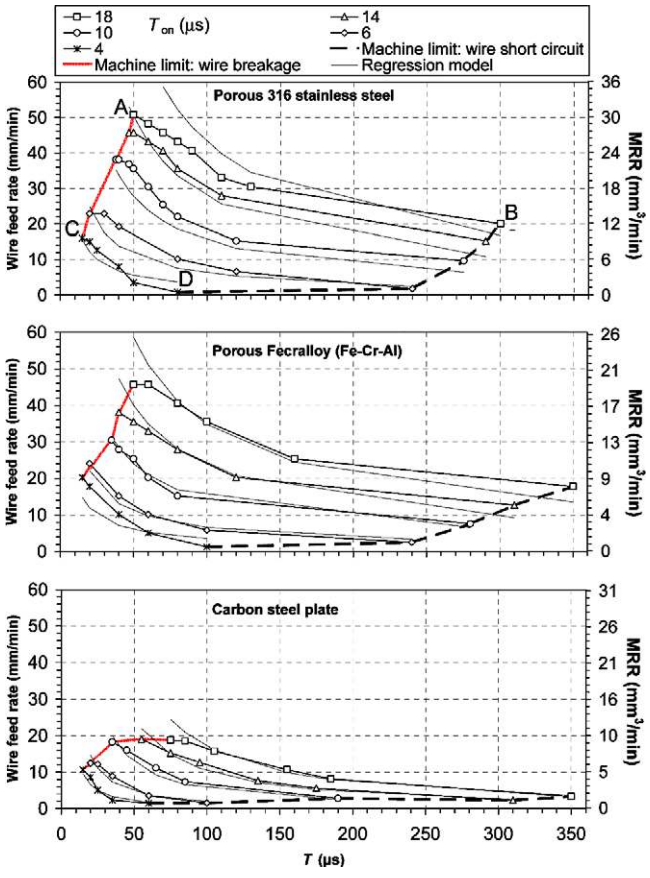

Fig. 5. Effects of T_{on} and T on wire feed rate for metal foams and carbon steel plate.

regions of frequent wire short circuit and breakage on both sides of the process envelope.

Using the wt% of the foam to calculate effective thickness, the maximum MRR for the 316 stainless foam, Fe-Cr-Al foam, and steel plate is calculated as 30.2, 19.6, and 9.74 mm^3/min, respectively. Experimental results show that, under the same EDM condition, the 316 stainless steel has higher MRR than the Fe-Cr-Al alloy. The melting temperature and electrical resistivity of Fe-Cr-Al and 316 stainless steel are 1500

and 1400 °C and 1.4 and 0.78 Ω-m, respectively. The lower melting temperature and electrical resistivity of 316 stainless steel contribute to its higher MRR. The carbon steel plate has relatively low MRR compared to the metal foams. This is likely due to better flushing conditions in the gap between the wire electrode and metal foam ligaments.

A model has been established to relate the wire feed speed, V_f, with T_{on} and T, for each set of wire EDM tests.

$$V_f = a \cdot \frac{T_{on}^b}{T^{b-c}} \tag{1}$$

The three parameters a, b, and c, can be obtained using linear regression analysis. This analysis tool uses the least squares method to fit a line through a set of experimental data. This tool enables the analysis of how a single dependent variable, V_f, is affected by the values of one or more independent variables, T_{on} and T. Table 1 lists the results of a, b, and c for these three materials and other wire EDM tests.

The thin lines in Fig. 5 are results predicted by the model. For most of the data points, the regression analysis model closely matches the experimental MRR data. At the corners and extreme T_{on} of the envelope, a larger deviation between the experimental data points and model prediction can be observed.

3.2. Metal-bond diamond grinding wheels

Fig. 6 shows a truing pass of the EDM wire moving across the surface of a rotating metal bond diamond grinding wheel at speed V_f. The mathematical formula to calculate the material removal rate for cylindrical wire EDM has been derived by Qu et al. [8]. The diameter of the wheel before and after the truing is denoted as D and d, respectively. The thickness of the layer removed from the grinding wheel is δ, which is set at about 0.15 mm in this study. The material removal rate can be expressed as:

$$\mathrm{MRR} = \frac{\pi(D^2 - d^2)V_f}{4} \tag{2}$$

where MRR is the material removal rate.

Effects of T_{on} and T on MRR for two metal bond diamond wheels are shown in Fig. 7. Four sides of the envelope are the 6 and 18 μs T_{on} and the wire short circuit and breakage limits. Machining at the 4 μs T_{on} does not produce spark energy density high enough to enable cutting. Diamond wheel I and II has the 320 and 1200 ANSI mesh size diamond grit, respectively. Both wheels are bronze bonded but have different compositions. The overall trend of MRR vs. T_{on} and T is similar for both grinding wheels. Compared to grinding wheel II, wire EDM machining of grinding wheel I exhibits higher MRR under the same set of process parameters. The peak MRR for grinding wheel I and II is 27.0 and 23.5 mm^3/min, respectively, comparable to that of the metal foams and higher than the carbon steel plate.

Regression analysis has been applied to model the MRR data. Results of three parameters a, b, and c are listed in Table 1.

3.3. Sintered Nd-Fe-B permanent magnet

Fig. 8 shows the wire feed rate and MRR vs. T at 6, 10, 14, and 18 μs T_{on} for wire EDM of sintered Nd-Fe-B magnet. The 2 and 4 μs T_{on} setup are not possible to achieve steady-state cutting conditions. A typical envelope is produced with four sides constrained by T_{on} upper and lower limits and wire short circuit and breakage limits. The highest MRR was 18 mm^3/min.

The MRR model obtained from regression analysis matches closely with the experimental data for the sintered Nd-Fe-B magnet. Table 1 lists results of the three parameters a, b, and c. Table 1 shows an interesting finding in that the parameter b/c falls into three levels depending on the type of work-material. For porous metal foam, solid material (carbon steel and Nd-Fe-B plate), and grinding wheel, b/c is about 1.9, 2.5, and 1.4, respectively. The percentage of difference of b/c

Table 1
Regression analysis results for wire EDM material removal rate model

Type of material and operation	Material	$a(\times 10^{-3})$	b	c	b/c	b/c % difference
Porous metal foam, slicing	Fe-Cr-Al foam	13.1	1.513	0.762	1.99	2.03
	316 stainless steel foam	4.15	1.763	0.90	1.95	
Solid material, slicing	Carbon steel plate	2.11	1.97	0.718	2.74	11.58
	Nd-Fe-B magnet	1.10	1.381	0.565	2.44	
Metal bond diamond wheel, rotary	Grinding wheel I	0.984	1.563	1.098	1.42	3.46
	Grinding wheel II	0.0910	1.92	1.303	1.47	

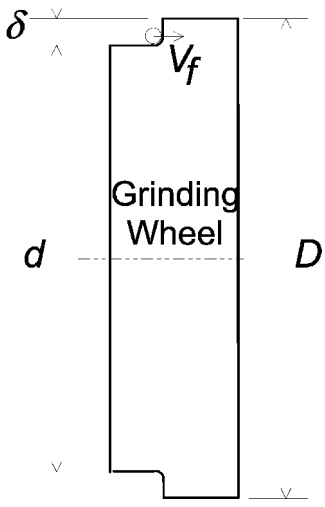

Fig. 6. Wire EDM of a metal bond diamond wheel.

relative to the average b/c of the two work-materials in the same group is also listed in Table 1.

3.4. Carbon–carbon bipolar plate

The wire feed rate vs. T at 4, 6, 10, 14, and 18 μs T_{on} for wire EDM of carbon–carbon bipolar plate is shown in Fig. 9. In all but the 4 μs T_{on}, the maximum slide speed of the machine, 305 mm/min, was the upper limit of the wire EDM envelope. This corresponds to 231 mm^3/min MRR, much higher than all the other

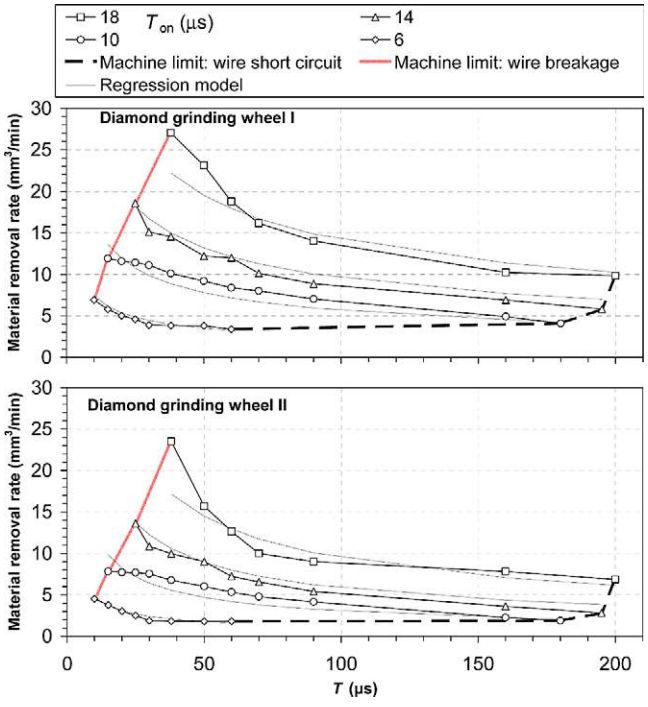

Fig. 7. Effects of T_{on} and T on wire feed rate of two metal bond diamond wheels.

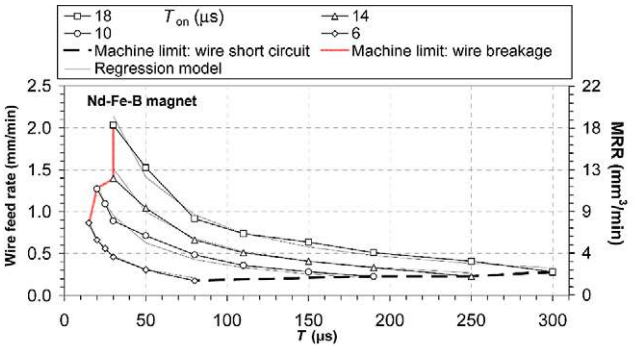

Fig. 8. Effects of T_{on} and T on wire feed rate for sintered Nd-Fe-B permanent magnet.

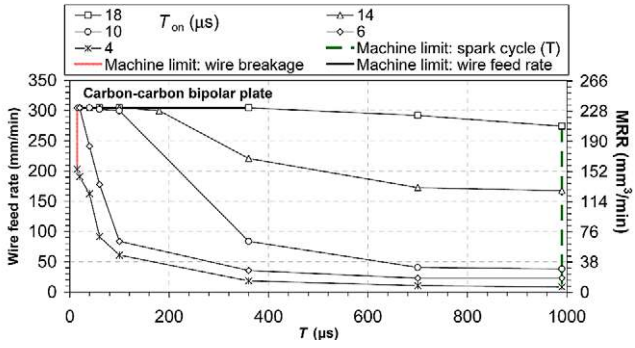

Fig. 9. Effects of T_{on} and T on wire feed rate for carbon–carbon bipolar plate.

materials investigated in this study. The low electrical resistance and low melting temperature of the carbon–carbon material contribute to such high MRR. Very high MRR was achieve at 18 μs T_{on} even at very high T. The envelope is enclosed by five boundary constraints: the upper and lower limits of T_{on}, the maximum machine slide speed limit, the wire breakage limit, and the maximum machine spark cycle, T, limit. The 1000 μs limit on T is unique in EDM machining of this material.

The MRR model in Eq. (1) was tested and found not suitable to model the carbon–carbon bipolar plate MRR. It is possible that the feed speed and machine performance, instead of material characteristics such as melting temperature, dominates the EDM material removal rate for this material.

4. Surface integrity

Selection of process conditions determines efficiency and MRR in EDM. Machining at high MRR requires high energy density spark erosion and generally causes low surface integrity. This section presents the qualitative analysis of effects of EDM process parameters on surface integrity. Machining with increased T_{on} and

T_{on}/T causes rougher surfaces [9]. The SEM and contact stylus profilometer for surface roughness measurement are used to examine samples of porous metal foams, carbon–carbon bipolar plate, and metal bond diamond wheels machined by EDM at different process settings.

4.1. Metal foams

Surfaces on the ligaments of two porous metal foams, 316 stainless steel and Fe-Cr-Al alloy, machined by EDM were examined using the SEM. Sample surfaces at four corners of the envelope, marked as A, B, C, and D on Fig. 5, were examined. These four samples represent four extreme cases of process conditions under either the wire breakage or short circuit and the longest or shortest T_{on}. Significantly different MRR at the lowest and highest level are also represented by these four samples.

SEM micrographs of the 316 stainless steel foam are shown in Fig. 10(a)–(d). Fig. 10(a) and (b) correspond to T_{on}= 18 μs. Bigger craters due to larger amount of molten work-material at each spark erosion can be identified on EDM surfaces. These two surfaces also correspond to have larger MRR. The crater size is reduced drastically on surfaces machined with T_{on}= 4 μs, as shown in Fig. 10(c) and (d). The surface area on the foam ligament is too small for contact surface roughness measurement.

4.2. Nd-Fe-B magnet

Fig. 11(a)–(c) show the surface and its close-up view of the sintered Nd-Fe-B magnet machined by EDM at T_{on} = 18, 10, and 2 μs. The thickness of the sample cut by wire EDM is 1.5 mm. In comparison, the thickness of Nd-Fe-B magnet used for the MRR experiment in Fig. 8 was 27 mm. Different levels of surface recast layer and damage can be observed on the EDM surface. Average surface roughness values, R_a, for T_{on} of 18, 10, and 2 μs are 4.0, 2.7, and 0.84 μm. This trend of lower T_{on} for better surface roughness is consistent with the previous research [9]. At long T_{on}= 18 μs, the amount of molten material deposit from each spark erosion is more significant than the other two EDM condition (T_{on} = 10 and 2 μs). On the surface with slow MRR (T_{on} = 2 μs in Fig. 11(c)), surface cracks possible due to thermal stress on the very brittle Nd-Fe-B material can be identified. The cavity, which can be seen in the close-up view in Fig. 11(b) and (c), is likely the inherent porosity during sintering Nd-Fe-B powder to produce the magnet. In Fig. 11(c), it is likely that each small hump, about 10 μm in size, is due to an individual spark erosion and deposition. This illustrates the low MRR and the type of surface damage for EDM brittle material.

4.3. Carbon–carbon bipolar plate

The SEM micrographs of the molded and EDM carbon–carbon bipolar plate surface are shown in Fig. 12.

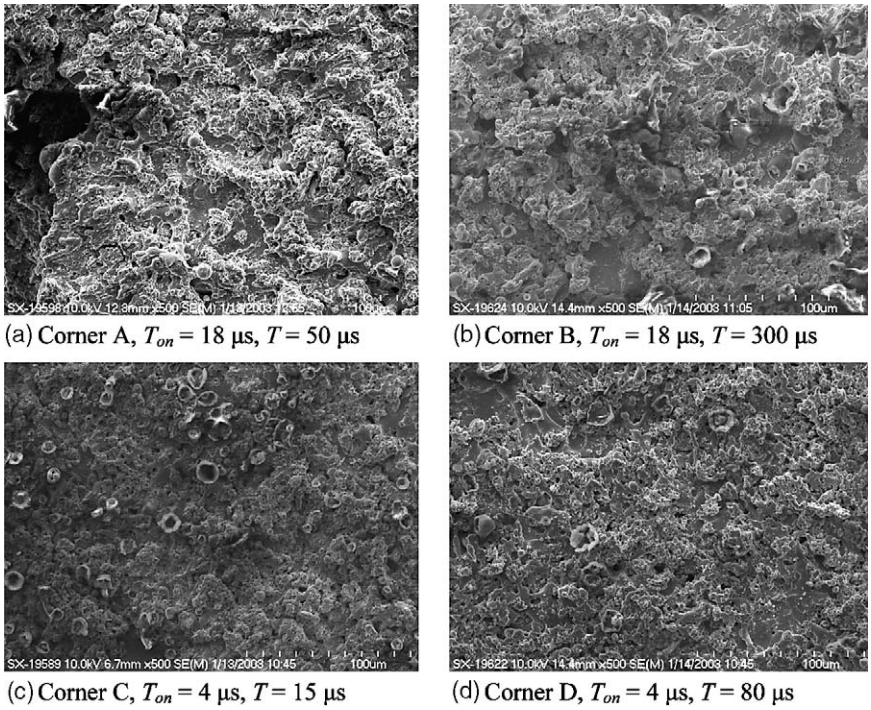

Fig. 10. SEM micrographs of 316 stainless steel foam surface machined by EDM.

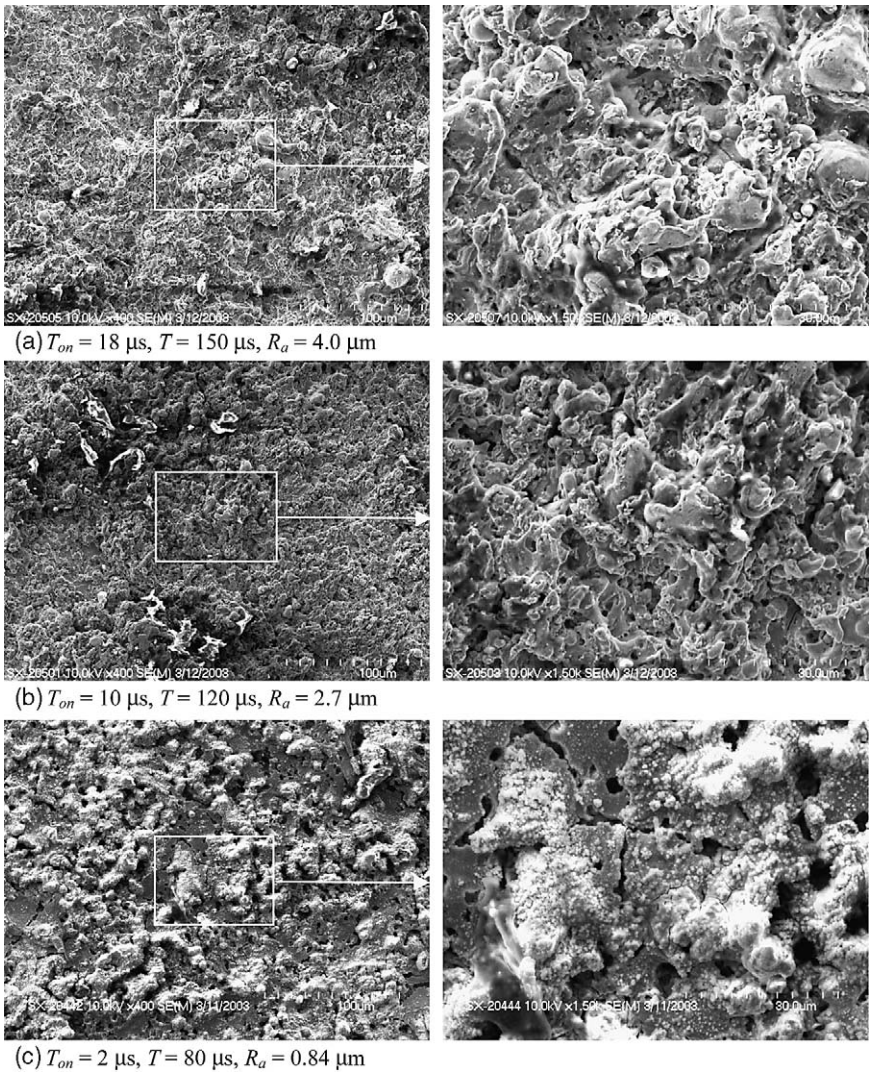

Fig. 11. SEM micrographs of Nd-Fe-B magnet surface machined by EDM.

The molded surface is shown in Fig. 12(a). In the production of the carbon–carbon bipolar plate, slurry molding of carbon fibers, about 0.4 mm long and 0.01 mm in diameter, was first performed and then followed by the chemical vapor-infiltration of carbon to seal the cavities.

Due to the high cutting speeds achievable by EDM of carbon–carbon bipolar plate, relatively high surface roughness of this material compared to others in this study is observed. Under SEM, the EDM surface of carbon–carbon bipolar plate machined under different process parameter settings yielded similar topography. A representative surface machined at $T = 14$ μs and $T_{on} = 180$ μs is illustrated in Fig. 12(b). The EDM machined surface is much rougher than that of molded surface. The R_a for molded and EDM cut surfaces is 1.40 and 15.5 μm, respectively. This confirms the observation in Fig. 12 of the rough EDM surface. The carbon fiber on EDM cut surface in Fig. 12(b) is not as apparent as in Fig. 12(a). The EDM process has melted the carbon fibers and sealing carbon and recast them to the surface. This can be recognized in the close-up view in Fig. 12(c).

4.4. Metal bond diamond grinding wheel

Fig. 13(a)–(d) show EDM trued surface of diamond grinding wheel II. A small segment was removed from the grinding wheel to be examined using the SEM for the EDM surfaces [10]. Three samples along the wire breakage boundary line of the process envelope shown in Fig. 7 were selected for the SEM and profilometer analysis. These three samples represent T_{on} of 18, 14, and 6 μs. The size of the craters and surface roughness decreases as T_{on} decreases. Lower T_{on} also corresponds to lower MRR. The arithmetic average roughness R_a

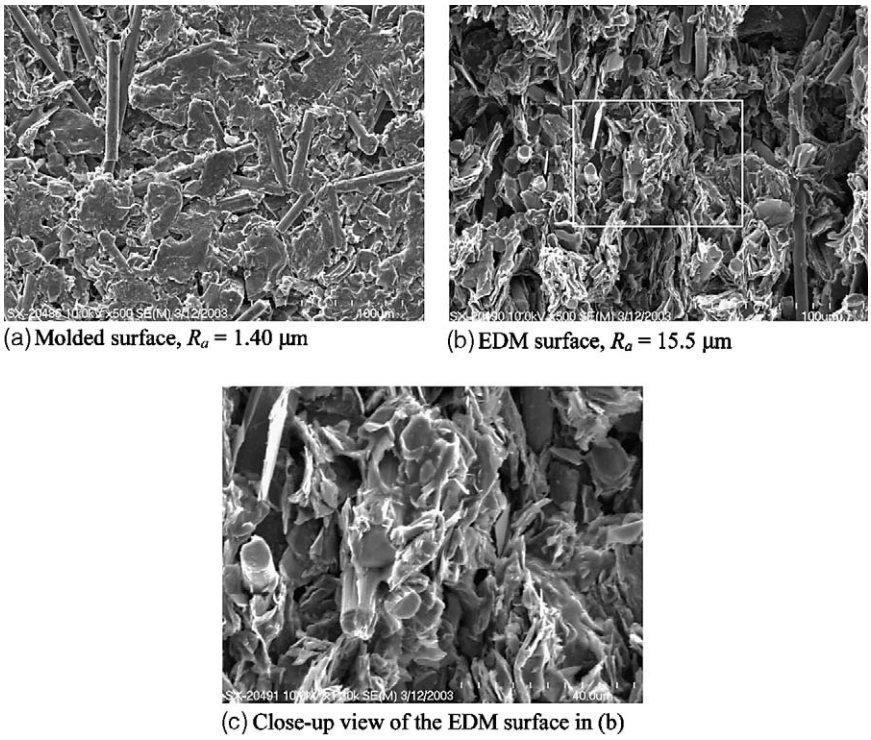

Fig. 12. SEM micrographs of molded and EDM (T = 180 μs, T_{on} = 14 μs) carbon–carbon bipolar plate.

for T_{on} of 18, 14, and 6 μs is 3.83, 2.86, and 2.15 μm, respectively. The protrusion of diamond grits, about 8 μm in size, and recast surface on the EDM surface with T_{on} = 18 μs can be recognized in Fig. 13(d).

5. Concluding remarks

The effects of spark cycle and pulse on-time on wire EDM of metal foams, metal bond grinding wheels, sintered Nd-Fe-B magnet, and carbon–carbon bipolar

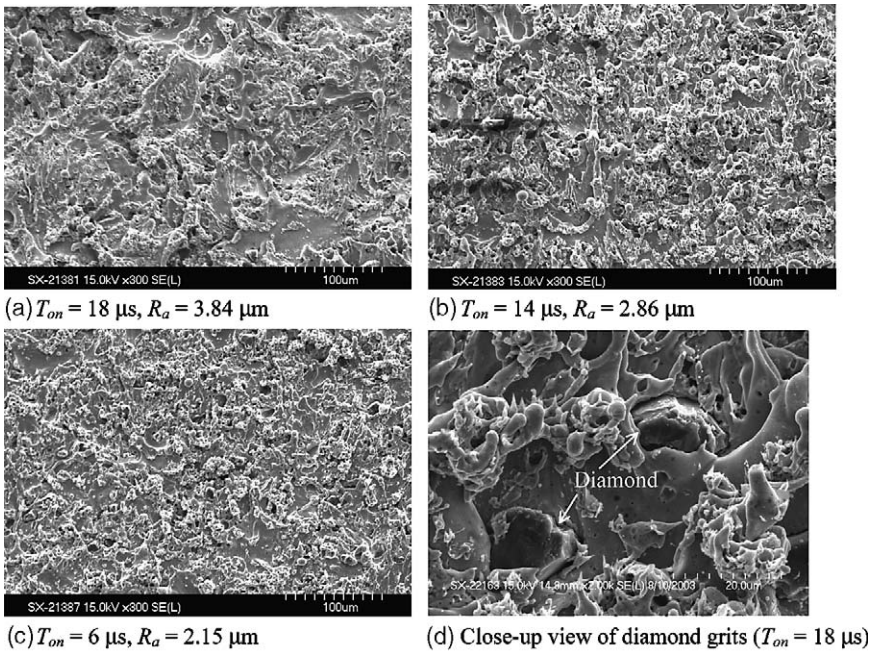

Fig. 13. SEM micrographs of metal bond diamond wheel I surface machined by EDM along the boundary line of wire breakage.

plate were investigated. An envelope of feasible EDM process parameters was generated for each work-material. Results were mutually compared in this study. Regression analysis was applied to model the wire EDM MRR. SEM analysis was used to investigate effect of important EDM process parameters on surface finish.

Although results presented are machine-dependent, this research provides the guidelines and procedures for the development of wire EDM process for machining new engineering materials to achieve different manufacturing objectives, either the high MRR, miniature features, or a compromise between the two.

This study also demonstrated the capability of wire EDM process to machine different advanced materials. Using traditional metal cutting methods, it is difficult to machine the metal foams without damaging the ligaments. The diamond grinding wheel is very difficult to machine to the precise shape. Sintered Nd-Fe-B magnet material is very brittle and easily chipped by using traditional machining methods. Carbon–carbon bipolar plate is delicate but can be machined easily by the EDM. The future research is to apply the envelope developed in this study for machining of miniature features and for high MRR EDM of advanced materials.

Acknowledgements

The authors acknowledge Magnequench and Dr. B. M. Ma for the sintered Nd-Fe-B permanent magnets, Porvair PLC and Dr. K. Butcher for the metal foam and carbon–carbon bipolar plate, and Cummins Inc. and D. J. Gust for the diamond grinding wheels. Part of this research was sponsored by the Assistant Secretary for Energy Efficiency and Renewable Energy, Office of Transportation Technologies, as part of the High Temperature Materials Laboratory User Program, Oak Ridge National Laboratory, managed by UT-Battelle, LLC for the US Department of Energy under contract number DE-AC05-00OR22725.

References

[1] C.C. Wang, B.H. Yan, Blind-hole drilling of Al_2O_3/6061Al composite using rotary electro-discharge machining, Journal of Materials Processing Technology 102 (2000) 90–102.

[2] C.L. Lin, J.L. Lin, T.C. Ko, Optimization of the EDM process based on the orthogonal array with fuzzy logic and grey relational analysis method, International Journal of Advanced Manufacturing Technology 19 (2002) 271–277.

[3] J.L. Lin, C.L. Lin, The use of the orthogonal array with grey relational analysis to optimize the electrical discharge machining process with multiple performance characteristics, International Journal of Machine Tools and Manufacture 42 (2002) 237–244.

[4] Y. Uno, A. Okada, Y. Okamoto, Y. Kazuo, S.H. Risbud, Y. Yamada, High efficiency fine boring of monocrystalline silicon ingot by electrical discharge machining, Precision Engineering 23 (1999) 126–133.

[5] K. Tsai, P. Wang, Comparison of neural network models on material removal rate in electrical discharge machining, Journal of Materials Processing Technology 117 (2001) 111–124.

[6] S.H. Lee, X.P. Li, Study of the effect of machining parameters on the machining characteristics in electrical discharge machining of tungsten carbide, Journal of Materials Processing Technology 115 (2001) 344–358.

[7] H. Hocheng, W.T. Lei, H.S. Hsu, Preliminary study of material removal in electrical-discharge machining of SiC/Al, Journal of Materials Processing Technology 63 (1997) 813–818.

[8] J. Qu, A.J. Shih, R.O. Scattergood, Development of the cylindrical wire electrical discharge machining process: Part I: Concept, Design and material removal rate, ASME Journal of Manufacturing Science and Engineering 124 (3) (2002) 702–707.

[9] J. Qu, A.J. Shih, R.O. Scattergood, Development of the cylindrical wire electrical discharge machining process: Part II: Surface integrity and roundness, Journal of Manufacturing Science and Engineering 124 (4) (2002) 708–714.

[10] B.K. Rhoney, A.J. Shih, R.O. Scattergood, J.L. Akemon, D.J. Gust, M.B. Grant, Cylindrical wire electrical discharge machining of metal bond diamond wheels for ceramic grinding, International Journal of Machine Tool and Manufacture 42 (2002) 1355–1362.

[11] M.F. Ashby, A. Evans, N.A. Fleck, L.J. Gibson, J.W. Hutchinson, H.N.G. Wadley, Metal Foams—A Design Guide, Butterworth-Heinemann, 2000.

[12] J. Banhart, Manufacture, characterization and application of cellular metals and metal foams, Progress in Material Science 46 (2001) 559–632.

[13] T.M. Besmann, J.W. Klett, J.J. Henry, E. Lara-Curzio, Carbon/carbon composite bipolar plate for proton exchange membrane fuel cells, Journal of the Electrochemical Society 147 (2000) 4083–4086.